Eur. Phys. J. B **53**, 39–45 (2006)
DOI: 10.1140/epjb/e2006-00341-4

THE EUROPEAN PHYSICAL JOURNAL B

Numerical study of the directed polymer in a 1 + 3 dimensional random medium

C. Monthus and T. Garel[a]

Service de Physique Théorique, CEA/DSM/SPhT, Unité de recherche associée au CNRS, 91191 Gif-sur-Yvette Cedex, France

Received 7 June 2006
Published online 6 September 2006 –

Abstract. The directed polymer in a $1+3$ dimensional random medium is known to present a disorder-induced phase transition. For a polymer of length L, the high temperature phase is characterized by a diffusive behavior for the end-point displacement $R^2 \sim L$ and by free-energy fluctuations of order $\Delta F(L) \sim O(1)$. The low-temperature phase is characterized by an anomalous wandering exponent $R^2/L \sim L^{\omega}$ and by free-energy fluctuations of order $\Delta F(L) \sim L^{\omega}$ where $\omega \sim 0.18$. In this paper, we first study the scaling behavior of various properties to localize the critical temperature T_c. Our results concerning R^2/L and $\Delta F(L)$ point towards $0.76 < T_c \leq T_2 = 0.79$, so our conclusion is that T_c is equal or very close to the upper bound T_2 derived by Derrida and coworkers (T_2 corresponds to the temperature above which the ratio $\overline{Z_L^2}/(\overline{Z_L})^2$ remains finite as $L \to \infty$). We then present histograms for the free-energy, energy and entropy over disorder samples. For $T \gg T_c$, the free-energy distribution is found to be Gaussian. For $T \ll T_c$, the free-energy distribution coincides with the ground state energy distribution, in agreement with the zero-temperature fixed point picture. Moreover the entropy fluctuations are of order $\Delta S \sim L^{1/2}$ and follow a Gaussian distribution, in agreement with the droplet predictions, where the free-energy term $\Delta F \sim L^{\omega}$ is a near cancellation of energy and entropy contributions of order $L^{1/2}$.

PACS. 02.50.-r Probability theory, stochastic processes, and statistics – 64.70.-p Specific phase transitions – 65.60.+a hermal properties of amorphous solids and glasses: heat capacity, thermal expansion, etc. – 05.40.-a Fluctuation phenomena, random processes, noise, and Brownian motion

1 Introduction

The model of a directed polymer in a random medium plays the role of a spin glass toy model in the field of disordered systems [1–5]. At low temperature, there exists a disorder dominated phase, where the order parameter is an 'overlap' [2,4,6,7]. In finite dimensions, a scaling droplet theory was proposed [5,8], in direct correspondence with the droplet theory of spin-glasses [9], whereas in the mean-field version of the model on the Cayley, a freezing transition very similar to the one occurring in the Random Energy Model was found [2]. The phase diagram as a function of space dimension d is the following [1]. In dimension $d \leq 2$, there is no free phase, i.e. any initial disorder drives the polymer into the strong disorder phase, whereas for $d > 2$, there exists a phase transition between the low temperature disorder dominated phase and a free phase at high temperature [10,11]. This phase transition has been studied exactly on a Cayley tree [2] and on hierarchical lattice [12]. In finite dimensions, bounds on the critical temperature T_c have been derived [11,13,14]: $T_0(d) \leq T_c \leq T_2(d)$. The upper bound $T_2(d)$ corresponds to the temperature above which the ratio $\overline{Z_L^2}/(\overline{Z_L})^2$ remains finite as $L \to \infty$. The lower bound T_0 corresponds to the temperature below which the annealed entropy becomes negative. On the Cayley tree, the critical temperature T_c coincides with T_0 [2]. In finite dimensions, there is a debate to know whether T_c coincides or not with T_2. Arguments in favor of the equality $T_c = T_2$ in finite dimensions d where $\omega(d) > 0$ can be found in [15], whereas a new upper bound T^* based on the entropy of random walks was recently proposed in [16]. As explained in detail in [17], the debate actually concerns the form of the negative tail of the free-energy distribution in the high temperature phase. If this tail decays only exponentially, as on the Cayley tree, then $T_c < T_2$ is possible; if it decays more rapidly than a simple exponential one gets $T_c = T_2$.

In this paper, we study numerically the scaling properties of the directed polymer in dimension $1+d$ with $d = 3$. As for previous numerical studies of the freezing transition in $d = 3$, we are only aware of references [13,21], which draw different conclusions for the specific heat exponent α, namely $\alpha \simeq -0.1 \pm 0.1$ in [13] and $\alpha = 2 - \nu \sim -2 \pm 0.7$ in [21]. With our numerical data, we are not able to give a reasonable quantitative estimate of this critical exponent (see below). However, our results concerning the scaling of the transverse displacement $R^2(L)$ and of the free-energy fluctuations $\Delta F(L)$ point towards a critical temperature T_c which is equal or very close to the upper bound T_2 discussed above. We also present histograms of free-energy,

[a] e-mail: garel@spht.saclay.cea.fr

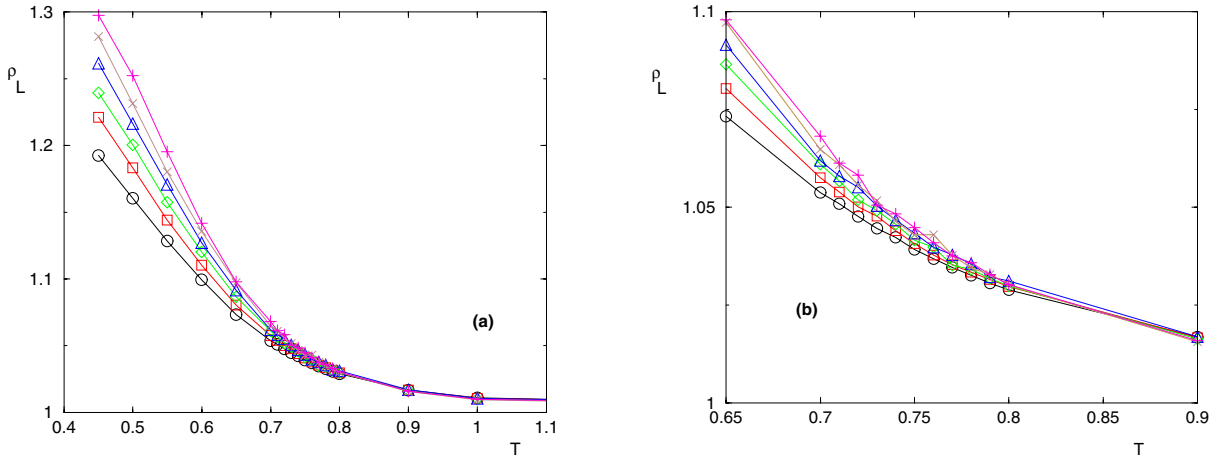

Fig. 1. (a) $\rho_L(T) = \overline{\langle R_L^2(T)\rangle}/L$ as a function of the temperature T for different $L = 30$ (◯), 36 (□), 42 (◊), 48 (△), 54 (×), 60 (+). (b) Zoom of the same data in the critical region.

energy and entropy as a function of temperature, in order to better understand the nature of the high and low temperature phases.

The paper is organized as follows. In Section 2, we define the model and give some numerical details. In Section 3, we present our results concerning the end-point fluctuations. In Section 4, we discuss the scaling behavior and the probability distribution of the free-energy, the energy and the entropy as T varies. In Section 5, we present the finite-size scaling analysis of spatial and thermodynamic observables. We summarize our conclusions in Section 6.

2 Model and numerical details

In this paper, we present numerical results for the random bond version of the model defined by the recursion relation on a cubic lattice in $d = 3$

$$Z_{L+1}(\vec{r}) = \sum_{j=1}^{2d} e^{-\beta\epsilon_L(\vec{r}+\vec{e}_j,\vec{r})} Z_L(\vec{r}+\vec{e}_j). \qquad (1)$$

The bond energies $\epsilon_L(\vec{r}+\vec{e}_j,\vec{r})$ are random independent variables drawn from the Gaussian distribution

$$\rho(\epsilon) = \frac{1}{\sqrt{2\pi}} e^{-\frac{\epsilon^2}{2}}. \qquad (2)$$

The numerical values of the bounds discussed in the Introduction are then given by [13]

$$T_0(d=3) = 0.528.. \leq T_c \leq T_2(d=3) = 0.790... \qquad (3)$$

In the previous numerical study of the same model [13], a finite size scaling analysis with respect to the transverse direction gave a critical temperature of order $T_c \sim 0.6$, whereas our data presented below point towards $T_c \sim T_2 = 0.79$.

In the high temperature phase ($T \geq T_c$), the free-energy density

$$f(T) \equiv -T \lim_{L\to\infty} \frac{\ln Z_L}{L} \qquad (4)$$

is known to coincide with the annealed value [3]

$$f(T) = f_{ann}(T) = -T\ln(2d) - \frac{1}{2T} \quad \text{for} \quad T \geq T_c. \qquad (5)$$

As a consequence, the energy $e(T)$ and the specific heat $c(T)$ also coincide with their annealed values $e_{ann}(T) = -1/T$ and $c_{ann}(T) = 1/T^2$, so that the regular parts of thermodynamic quantities can be exactly substracted out.

The numerical results presented in the following have been obtained from the direct iteration of the transfer matrix equation (1). In Section 3 concerning the end-point transverse fluctuations, we give results for lengths L in the range $30 \leq L \leq 60$, with $n_s(L)$ independent samples between $n_s(L=30) = 3.5\times10^5$ and $n_s(L=60) = 2.3\times10^4$. In Section 4 concerning thermodynamic quantities, we have used similar values, as well as smaller sizes to have a bigger range in the size L. For instance, the data presented in Figure 4 correspond to lengths $L = 6,\ 12,\ 24,\ 48$ with respective numbers $n_s(L)$ of independent samples of order $n_s(L) = 9\times10^6, 9\times10^6, 6\times10^5, 4\times10^4$.

3 Study of spatial properties

The phase transition corresponds to a change in the wandering exponent ζ characterizing the transverse fluctuations $\overline{\langle R_T^2(L)\rangle}$ of the end-point of the polymer [1]

$$\overline{\langle R_T^2(L)\rangle} \underset{L\to\infty}{\simeq} L \quad \text{for} \quad T \geq T_c \qquad (6)$$

$$\overline{\langle R_T^2(L)\rangle} \underset{L\to\infty}{\simeq} L^{2\zeta} \quad \text{for} \quad T < T_c \qquad (7)$$

where, as usual, $\langle A\rangle$ and $\overline{A}$ denote respectively thermal and disorder averages. The exponent $\zeta \sim 0.59...$ characterizes the zero-temperature fixed point [1]. In Figure 1,

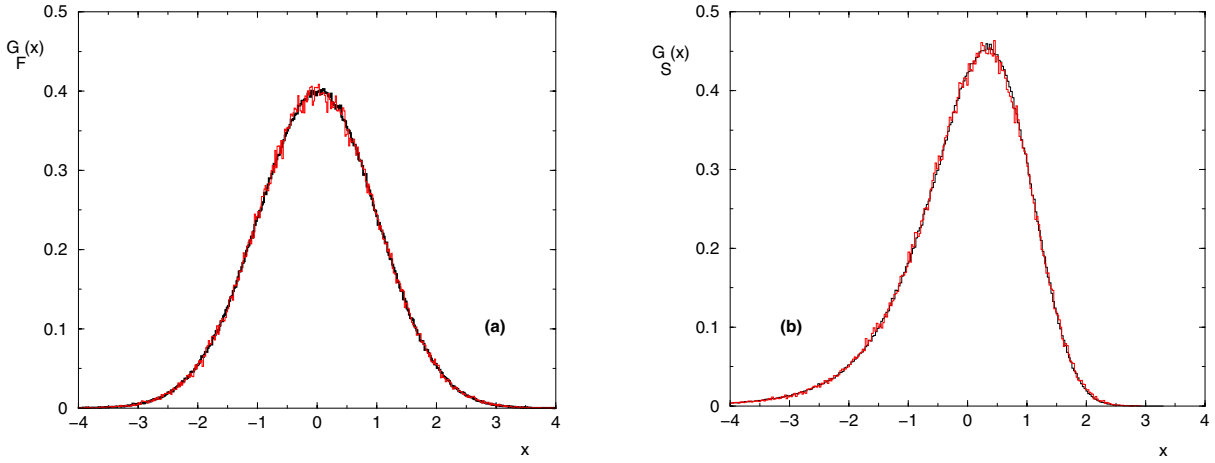

Fig. 2. High temperature phase: (a) Gaussian rescaled probability distribution $G_F(x)$ of the free energy at $T = 2$ for $L = 18,\ 30$. (b) Non-Gaussian rescaled probability distribution $G_S(x)$ of the entropy at $T = 2$ for $L = 18,\ 30$.

we show the data for $\rho_L(T) = \overline{\langle R_T^2(L)\rangle}/L$ as a function of the temperature T for increasing lengths in the range $30 \leq L \leq 60$. To localize the critical temperature T_c, we have tried to fit our data according to the following form

$$\frac{\overline{\langle R_T^2(L)\rangle}}{L} = a_0(T)L^{\omega} + a_1(T) + \frac{a_2(T)}{L} \qquad (8)$$

where we have used the scaling relation $\omega = 2\zeta - 1 \sim 0.186$. The coefficient $a_0(T)$ is found to vanish around $T_c \simeq 0.78$–0.79. A tentative finite-size scaling analysis is shown in Figure 8.

4 Study of thermodynamic properties

For a disordered sample (i) of length L, we note the free energy $F_T(L,i)$, the entropy $S_T(L,i)$ and the internal energy $E_T(L,i)$. For each of these observables $(X = F, S, E)$, we will discuss the behavior of the averaged value $X_T^{av}(L)$, of the variance $\Delta X_T(L)$ and of the rescaled probability distribution

$$P_{(T,L)}(X) \simeq \frac{1}{\Delta X_T(L)}\, G\left(x = \frac{X - X_T^{av}(L)}{\Delta X_T(L)}\right). \qquad (9)$$

4.1 Delocalized phase at very high temperature $T \gg T_c$

In the high temperature phase $T \gg T_c$, the free-energy $F_T(L,i)$, the entropy $S_T(L,i)$ and the energy $E_T(L,i)$ of a sample (i) of length L are expected to be

$$F_T(L,i) = Lf_{ann} + a_i \qquad (10)$$
$$S_T(L,i) = Ls_{ann} + b_i \qquad (11)$$
$$E_T(L,i) = Le_{ann} + c_i \qquad (12)$$

where a_i, b_i, c_i are random variables of order $O(1)$. The rescaled distribution (9) of the free energy is found to be Gaussian (see Fig. 2a), whereas the rescaled probability distribution of the entropy is asymmetric (see Fig. 2b).

4.2 Localized phase at very low temperature $T \ll T_c$

Let us first recall some theoretical expectations. At $T = 0$, the ground state energy of a sample (i) of size L takes the scaling form

$$E_0(L,i) = Le_0 + L^{\omega}u_i \qquad (13)$$

where u_i is a random variable of order $O(1)$. As a consequence, both the correction to extensivity and the fluctuations involve the same exponent $\omega \sim 0.186$

$$\overline{E_0(L,i)} - Le_0 \ = L^{\omega}\overline{u_i} \qquad (14)$$
$$\Delta E_0(L) \ = L^{\omega}\left(\overline{u_i^2} - (\overline{u_i})^2\right)^{1/2}. \qquad (15)$$

Numerical results on the statistical properties of the ground state and low energy excitations are discussed in our recent work [22]. According to the droplet theory, the whole low temperature phase $0 < T < T_c$ is governed by a zero-temperature fixed point. However, many subtleties arise because the temperature is actually 'dangerously irrelevant'. The main conclusions of the droplet analysis [5] can be summarized as follows. The scaling (13) translates into the statistical properties of the free energy, provided one introduces a correlation length $\xi(T)$ to rescale the length L

$$F_T(L,i) - Lf_{ann} = \left(\frac{L}{\xi(T)}\right) + f_1(T)\left(\frac{L}{\xi(T)}\right)^{\omega} u_i \qquad (16)$$

where u_i is a random variable of order $O(1)$.

For T low enough $(T \leq 0.4)$, we find that the width $\Delta F(L,T)$ indeed scales as $L^{0.18}$. Moreover the rescaled distribution (9) coincides with the rescaled distribution of the ground state energy at $T = 0$ (see Fig. 3a).

However, within the droplet theory [5], the random part of order L^{ω} of the free-energy (Eq. (16)) is expected to be a near cancellation of energy and entropy random contributions of order $L^{1/2}$. The argument is that the energy and entropy are dominated by small scale contributions of random sign [5], whereas the free energy is optimized on the coarse-grained scale $\xi(T)$. These predictions

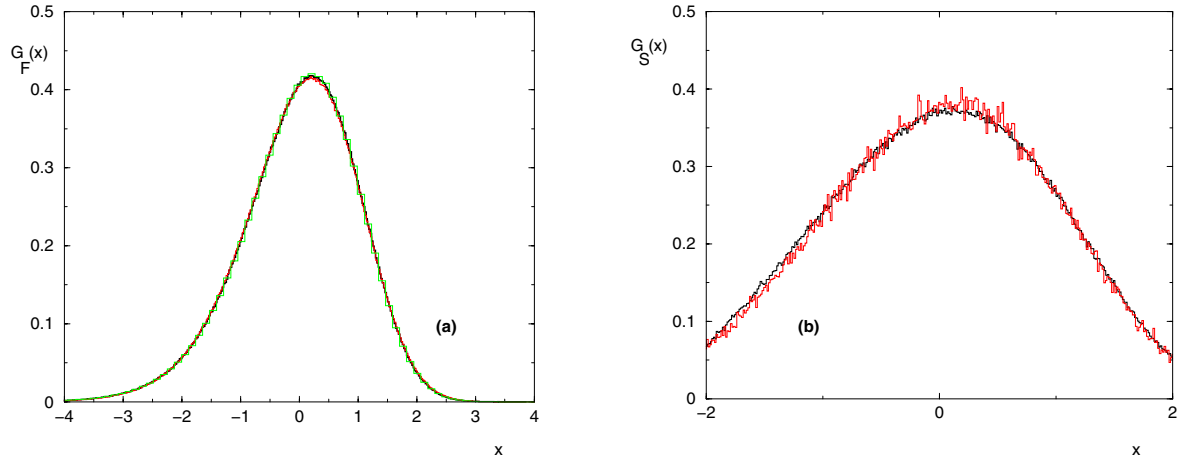

Fig. 3. (a) $T = 0$ fixed point: comparison of the rescaled distributions of the ground state energy $G_{E_0}(x)$ and of the free energy $G_F(x)$ at $T = 0.25,\ 0.4$ for $L = 12$ (b). The rescaled entropy distribution $G_S(x)$ for $T = 0.25$ and $L = 18,\ 30$ is found to be Gaussian in agreement with the droplet picture.

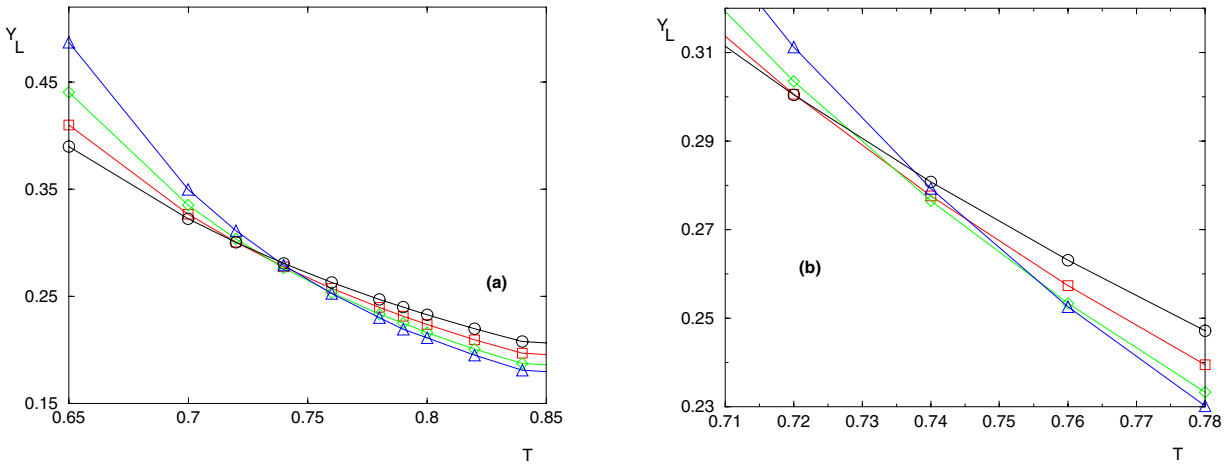

Fig. 4. (a) Plot of $Y_L(T) = \frac{F_T^{av}(L) - L f_{ann}}{(\ln L)^{1/2}}$ for $L = 6$ (◯), 12 (□), 24 (◊), 48 (△). (b) Zoom around the pseudo-crossing point, showing a systematic shift with L: the curves for $L = 6$ and $L = 12$ cross around $T \sim 0.72$, whereas the curves for $L = 24$ and $L = 48$ cross around $T \sim 0.755$.

for the energy and entropy have been numerically checked in $d = 1$ and $d = 2$ [5,23]. Moreover, the droplet argument [5] suggests that the entropy can be written as

$$S_T(L, i) - L s_{ann} = s_0(T)L + s_1(T)L^{1/2} v_i + \ldots \quad (17)$$

where v_i is Gaussian, because the entropy is dominated by a large number of independent local excitations. We show in Figure 3b that the rescaled distribution is in good agreement with this argument.

Then from the thermodynamic relation $F = E - TS$, the energy is expected to have a more complicated form involving terms of order L, $L^{1/2}$ and L^{ω}.

4.3 Critical region

4.3.1 Free-energy scaling at T_c

At T_c, the wandering exponent ζ is expected to be exactly $\zeta_c = 1/2$ [24], and thus the scaling relation $\omega_c = 2\zeta_c - 1$ between exponents [25] yields $\omega_c = 0$. Previous numerical studies and arguments [21,26] have concluded that the free-energy is logarithmic at T_c with exponent (1/2)

$$F_{T_c}(L, i) - L f_{ann} = (\ln L)^{1/2} w_i \quad (18)$$

where w_i is a random variable of order $O(1)$. We show in Figure 4a that the rescaled variable $Y_L(T) = \frac{F_T^{av}(L) - L f_{ann}}{(\ln L)^{1/2}}$ increases with L in the low temperature phase, and decreases with L in the high temperature phase. In the critical region, there is a systematic shift in the crossing points of curves when L increases (see the zoom of Fig. 4b). Since our numerical data are not sufficient to analyse quantitatively the L-dependence of this shift, we simply conclude that the thermodynamic critical temperature T_c is in the region $T_c \geq 0.76$, and is thus very close to the exact upper bound $T_2 = 0.79$ (Eq. (3)).

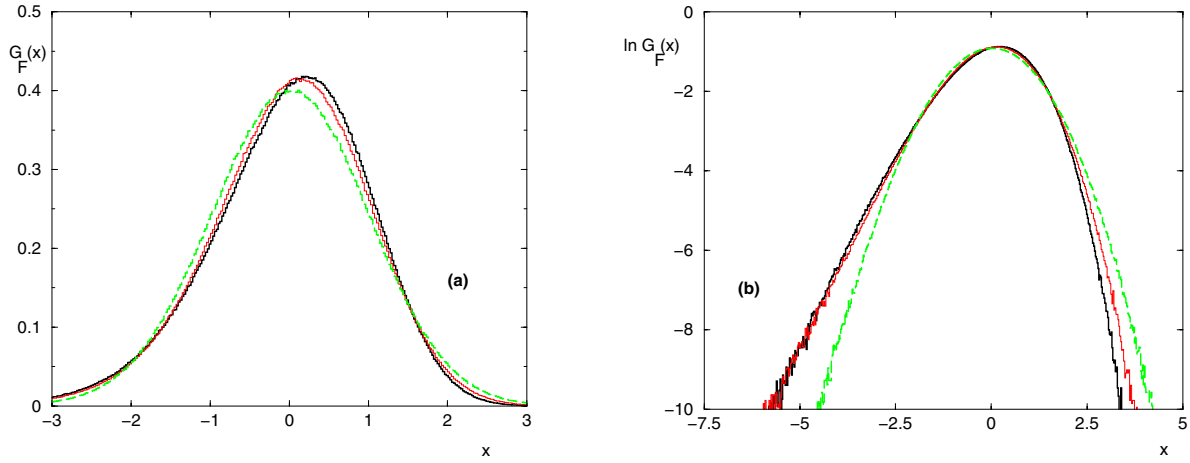

Fig. 5. Free energy distribution: (a) rescaled probability distribution $G_F(x)$ of the free-energy for $L = 12$ in the low temperature phase $T = 0.25$ (thick line), in the high temperature phase $T = 2$ (Gaussian, long dashed line) and in the critical region $T = 0.79$ (thin line). (b) Logarithmic plot of the same data: in the critical region, the negative tail is very close to the low-temperature tail and far from the Gaussian high temperature tail.

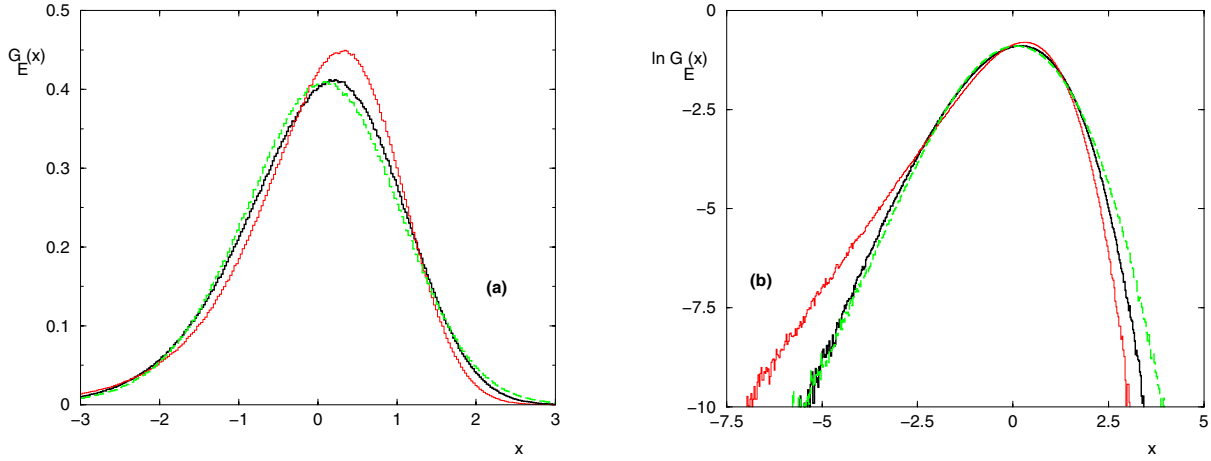

Fig. 6. (a) Rescaled energy distributions for $L = 12$ in the low temperature phase $T = 0.25$ (thick line), in the high temperature phase $T = 2$ (long dashed line) and in the critical region $T = 0.79$ (thin line), where the distribution is maximally peaked. (b) Logarithmic plot of the same data: the slower decay in the negative tail is obtained in the critical region and seems to correspond to an exponential decay $\ln G_E(x) \sim -|x|$ near T_c.

4.3.2 Rescaled distributions of free energy, energy and entropy in the critical region

In this section, we compare the rescaled probability distributions of thermodynamic observables in the critical region with respect to the low temperature and high temperature corresponding results.

The results for the free-energy are shown in Figures 5 focusing on the bulk (a) and on the tails (b). The negative tail of this probability distribution is of particular interest, since it is linked to the location of the critical temperature T_c with respect to the upper bound T_2 as explained in details in [17]. If this tail is exponential $G_F(x) \sim e^{-a|x|}$ for $x \to -\infty$ as on the Cayley tree [2], then $T_c < T_2$, whereas if $G_F(x)$ decays more rapidly than exponentially, then $T_c = T_2$. For instance, in the mean-field Sherrington-Kirkpatrick model of spin-glasses, one has $T_c = T_2$ and the distribution of the free-energy fluctuations for $T > T_c$ is known to be Gaussian [18,19]. Here we obtain numerically that $G_F(x)$ is Gaussian in the high temperature phase for $T \gg T_2$ (see Fig. 2a). If this Gaussian distribution is valid in the whole high temperature phase, then one has the equality $T_c = T_2$. On the other hand, the strict inequality $T_c < T_2$ requires that the negative tail becomes exponential in a region above T_c. Such a 'transition' in the form of the free-energy distribution within a high temperature phase is known to exist for instance in the Random Energy Model [20]. Here with our numerical results, as T grows from T_2 to $T \gg T_2$, we see a slow crossover from the low-temperature tail towards the Gaussian high temperature tail (see Fig. 5). Since $G_F(x)$ decays in the low-temperature phase as $e^{-b|x|^\eta}$ with $\eta = 1/(1-\omega) > 1$ according to Zhang argument [1,15,17], we see no sign of an exponential decay with power $\eta = 1$ at any temperature.

The rescaled probability distribution for the energy and entropy are shown respectively in Figures 6 and 7

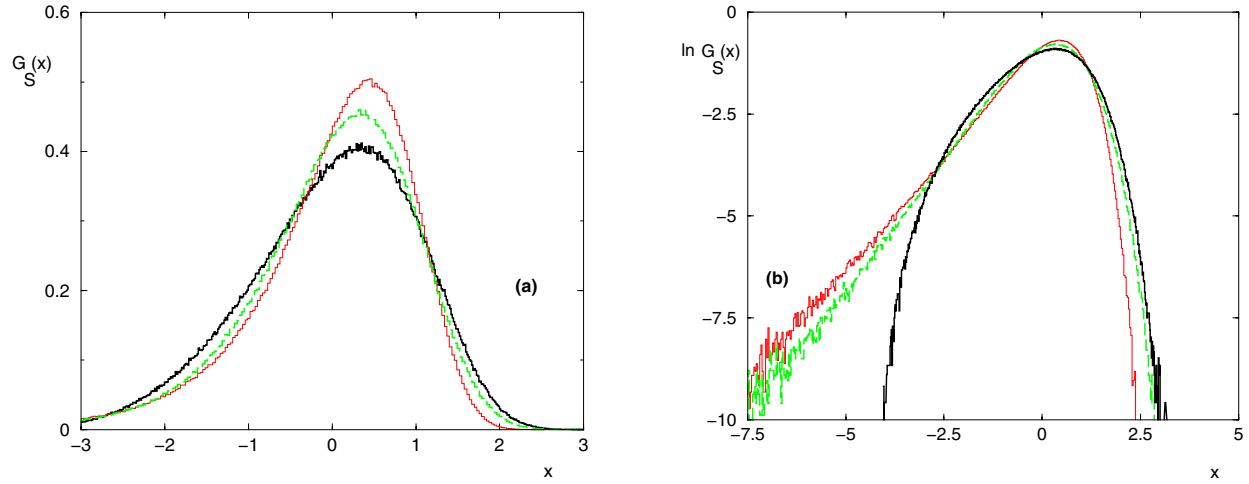

Fig. 7. (a) Rescaled entropy distributions for $L = 18$ in the low temperature phase $T = 0.4$ (thick line), in the high temperature phase $T = 2$ (long dashed line) and in the critical region $T = 0.79$ (thin line), where the distribution is maximally peaked. (b) Logarithmic plot of the same data: the slower decay in the negative tail is obtained in the critical region and seems to correspond to an exponential decay $\ln G_S(x) \sim -|x|$ near T_c.

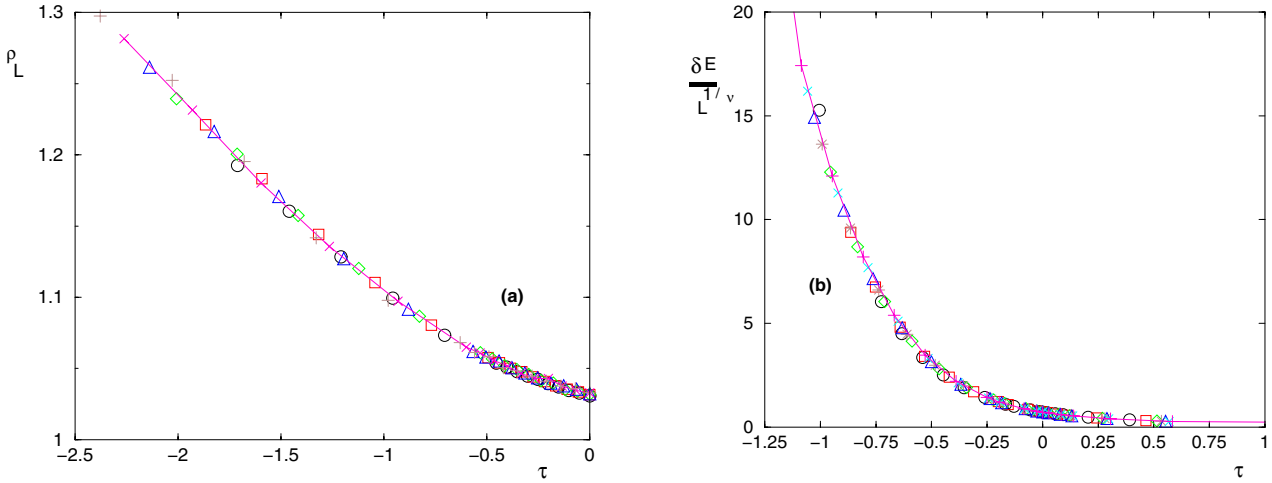

Fig. 8. (a) Plot of the data of Figure 1 for $\rho_L(T) = \overline{\langle R_L^2(T)\rangle}/L$, as a function of the rescaled variable $\tau = (T - T_c)L^{1/\nu}$, see equation (19), with $T_c = 0.79$ and $\frac{1}{\nu} \sim 0.475$. Symbols: $L = 30$ (◯), 36 (□), 42 (◊), 48 (△), 54 (×), 60 (+). (b) Plot of the rescaled energy $\frac{\delta E}{L^{1/\nu}}$ of equation (20) as a function of the rescaled variable $\tau = (T - T_c)L^{1/\nu}$, with $T_c = 0.79$ and $\frac{1}{\nu} \sim 0.25$. Symbols: $L = 12$ (◯), 24 (□), 36 (◊), 48 (△), 54 (×), 60 (+).

focusing on the bulk (a) and on the tails (b). Concerning the bulk (see Figs. 6a and 7a), both distributions have a non-monotonous behavior as T varies, and become maximally peaked in the critical region $0.7 < T < 0.9$. As for the negative tails (see Figs. 6b and 7b), the slower decay is obtained in the critical region and seems to correspond to an exponential decay $G_{E,S}(x) \sim e^{-c|x|}$.

5 Tentative finite size scaling analysis on averaged observables

Fixing the critical temperature at $T_c = T_2 = 0.79$, we have tried to make some finite-size scaling analysis to determine the value of the correlation length exponent ν, which is related to the specific heat exponent α via the hyperscaling relation $\nu = 2 - \alpha$.

We first consider the spatial properties discussed in Section 3. The best rescaling of the data of Figure 1a according to the finite size scaling form

$$\frac{\overline{\langle R_T^2(L)\rangle}}{L} = \Phi\left((T - T_c)L^{1/\nu}\right) \qquad (19)$$

corresponds to values in the range $0.45 < \frac{1}{\nu} < 0.5$, see Figure 8a.

We then consider the averaged energy, with the following usual finite-size scaling form

$$\delta E = E_T^{av}(L) - Le_{ann} = L^{1/\nu}\Psi\left((T - T_c)L^{1/\nu}\right). \qquad (20)$$

The best rescaling (see Fig. 8b) correspond to $0.23 < \frac{1}{\nu} < 0.27$.

These two values are clearly not compatible. Note that the same incompatible values have been found in previous studies [13,21]. This problem may have several reasons, such as the too small system sizes studied, or the applicability of finite size scaling to disordered systems [27]. As a consequence, we cannot give a reasonable quantitative estimate of the critical behavior. In this respect, we recall that an alternative to the usual power-law behavior $\xi(T) \sim (T_c - T)^{-\nu}$, has been proposed in reference [15], namely $\ln \xi(T) \sim \ln^2(T_c - T) + ...$ Unfortunately, our numerical data are not able to test this alternative form without any knowledge of subleading divergent terms.

6 Conclusion

In this paper, we have presented numerical results for the directed polymer in a 1 + 3 dimensional random medium. Our data concerning the wandering $R_T^2(L)$ of the end-point and the free energy $F_T(L)$ point towards $0.76 < T_c \leq T_2 = 0.79$, so our conclusion is that the critical temperature T_c is equal or very close to the upper bound T_2 derived by Derrida and coworkers. We have also presented results for histograms of free-energy, energy and entropy as T varies. For $T \gg T_c$, we obtain that the free-energy distribution is Gaussian. For $T \ll T_c$, the free-energy distribution coincides with the ground state energy distribution, in agreement with the zero-temperature fixed point picture, and the entropy fluctuations of order $\Delta S \sim L^{1/2}$ follow a Gaussian distribution, in agreement with the droplet predictions. However, from our various data, we cannot give a reasonable quantitative estimate of the divergence of the correlation length $\xi(T)$ as $T \to T_c^-$.

We thank H. Spohn for pointing out reference [16] to us.

References

1. T. Halpin-Healy, Y.-C. Zhang, Phys. Repts. **254**, 215 (1995)
2. B. Derrida, H. Spohn, J. Stat. Phys. **51**, 817 (1988)
3. B. Derrida, Physica A **163**, 71 (1990)
4. M. Mézard, J. Phys. France **51**, 1831 (1990)
5. D.S. Fisher, D.A. Huse, Phys. Rev. B **43**, 10728 (1991)
6. P. Carmona, Y. Hu, Prob. Th., Rel. Fields **124**, 431 (2002); P. Carmona, Y. Hu, e-print `arXiv:math.PR/0601670`
7. F. Comets, T. Shiga, N. Yoshida, Bernoulli **9**, No. 4, 705 (2003)
8. T. Hwa, D.S. Fisher, Phys. Rev. B **49**, 3136 (1994)
9. D.S. Fisher, D.A. Huse, Phys. Rev. B **38**, 386 (1988)
10. J.Z. Imbrie, T. Spencer, J. Stat. Phys. **52**, 609 (1988)
11. J. Cook, B. Derrida, J. Stat. Phys. **57**, 89 (1989)
12. B. Derrida, R.B. Griffiths, Europhys. Lett. **8**, 111 (1989)
13. B. Derrida, O. Golinelli, Phys. Rev. A **41**, 4160 (1990)
14. M.R. Evans, B. Derrida, J. Stat. Phys. **69**, 427 (1992)
15. C. Monthus, T. Garel, e-print `arXiv:cond-mat/0603041`
16. M. Birkner, Elect. Comm. in Probab. **9**, 22 (2004); M. Birkner, Ph.D. thesis, `http://publikationen.stub.uni-frankfurt.de/volltexte/2003/314/`
17. C. Monthus, T. Garel, e-print `arXiv:cond-mat/0605448`
18. M. Aizenman, J.L. Lebowitz, D. Ruelle, Comm. Math. Phys. **112**, 3 (1987)
19. F. Comets, J. Neveu, Comm. Math. Phys. **166**, 549 (1995)
20. A. Bovier, I. Kurkova, M. Löwe, Ann. Prob. **30**, 605 (2002)
21. J.M. Kim, A.J. Bray, M.A. Moore, Phys. Rev. A **44**, R4782 (1991)
22. C. Monthus, T. Garel, e-print `arXiv:cond-mat/0602200`
23. X-H. Wang, S. Havlin, M. Schwartz, J. Phys. Chem. B **104**, 3875 (2000); X-H. Wang, S. Havlin, M. Schwartz, Phys. Rev. E **63**, 032601 (2001)
24. C.A. Doty, J.M. Kosterlitz, Phys. Rev. Lett. **69**, 1979 (1992)
25. D.A. Huse, C.L. Henley, Phys. Rev. Lett. **54**, 2708 (1985)
26. B.M. Forrest, L.-H. Tang, Phys. Rev. Lett. **64**, 1405 (1990)
27. S. Wiseman, E. Domany, Phys. Rev. Lett. **81**, 22 (1998); S. Wiseman, E. Domany, Phys. Rev. E **58**, 2938 (1998)